Lumped Parameter Models for Building Thermal Modelling: An Analytic approach to simplifying complex multi-layered constructions

Alfonso P. Ramallo González[1,*], Matthew E. Eames[1], David A. Coley[2]

[1] *Department of Engineering, Mathematics and Physical Sciences, University of Exeter, UK.*

[2] *Department of Architecture and Civil Engineering, University of Bath, UK.*

[*] *Corresponding email: ar321@exeter.ac.uk*

Keywords: Lumped Parameter Models, Buildings, Thermal Simulations, Constructions, Dominant Layer Model, DLM.

SUMMARY

There are many sophisticated building simulators capable of accurately modelling the thermal performance of buildings. Lumped Parameter Models (LPMs) are an alternative which, due to their shorter computational time, can be used where many runs are needed, for example when completing computer-based optimisation. In this paper, a new, more accurate, analytic method is presented for creating the parameters of a second order LPM, consisting of three resistors and two capacitors, that can be used to represent multi-layered constructions. The method to create this LPM is more intuitive than the alternatives in the literature and has been named the *Dominant Layer Model.* This new method does not require complex numerical operations, but is obtained using a simple analysis of the relative influence of the different layers within a construction on its overall dynamic behaviour. The method has been used to compare the dynamic response of four different typical constructions of varying thickness and materials as well as two more complex constructions as a proof of concept. When compared with a model that truthfully represents all layers in the construction, the new method is largely accurate and outperforms the only other model in the literature obtained with an analytical method.

1 Introduction

Low-carbon policies and the increasing cost of energy is making society more aware of the need for low-energy solutions. The domestic sector accounts for around 30% of total energy demand in the UK, and it is responsible for around 27 % of all carbon emissions [1]. The domestic sector has been highlighted as one of the key vectors for reducing emissions [2]. Building models are fundamental tools used to investigate the thermal performance and energy use of a design. These models have the potential to be used for designing buildings that use less energy and that have a lower carbon footprint.

Currently several building simulators exist which are able to model most of the physical phenomena affecting buildings [3]. However, these simulators need a substantial computational time to perform a yearly simulation. When the user requires running a large number of simulations, these tools might not be ideal, as their use might render the study unfeasible due to prohibitive overall computational times. Some authors have faced this problem and used surrogate models to reduce the computational times (such as [4]) but others have used simpler simulators to represent buildings (such as [5], [6] or [7]).

Some of these simple simulators, developed in the seventies [8], use linear dynamic models to obtain the thermo-dynamic response of buildings. The linear dynamic models used are not capable to model radiation and convection, instead linear approximations are used to model these heat transfer mechanisms.

The equation of heat transfer through solids is, however linear, and can be represented with the so called electrical analogy when discretised in space. With this analogy, the conductivity of the materials is interpreted as electric conductivity, and the thermal mass as electrical capacity.

An example of a simulator using this electrical analogy was published by Balcomb et al. where the thermal behaviour of a building heated with solar gains is modelled with a simple network of resistors and capacitors (RC-network), that represent conductivities and thermal masses of the building [9].

The advantage of using RC-networks to represent buildings, is that they can be mathematically modelled by a set of first order differential equations, also called state-space systems (see [10]). The integration of these systems provides the variables of the model (temperatures of building elements and zones) at a relatively low computational cost. The short computational times made these models popular during the 70's when computational resources were limited. However they are still used when quick building simulators are needed to perform a large number of simulations [5-7].

Constructing building models with RC-networks implies representing every element of the building with resistors and capacitors. This is also the case with multi-layered constructions. Each slab of material in a multi-layered construction has to be represented in the RC-network, with at least two resistors, one capacitor and one internal node [11] (see Figure 1a). Including all the layers in the construction for all the surfaces of the envelope leads to large RC-networks; to integrate the set of differential equations of a state-space system the time is discretised using a time step and the variables can be obtained using Eq. 1.

$$x_{n+1} = e^{A\Delta t}\ x_n + Ku, \tag{1}$$

where x_{n+1} and x_n are vectors representing the variables in time step $n+1$ and n, u is the vector of inputs, and $e^{A\Delta t}$ and K are calculated matrices to integrate the state-space system [10]. The vector of variables (x_n) has to be multiplied for the matrix $e^{A\Delta t}$ in every time step and so has to be done with matrix K and u. The matrix $e^{A\Delta t}$ could be calculated once for the whole year simulation; however, the multiplications previously mentioned have to be performed in every time step, meaning that there exists a high potential for reducing the computational time of the simulation by reducing the size of these matrices. This can be done by reducing the number of nodes of the RC-network i.e. creating a Lumped Parameter Model (LPM). As an example, the reduction of an RC-network with 12 nodes to a simplified LPM with 3 nodes will make the computational time of every time step 16 times shorter.

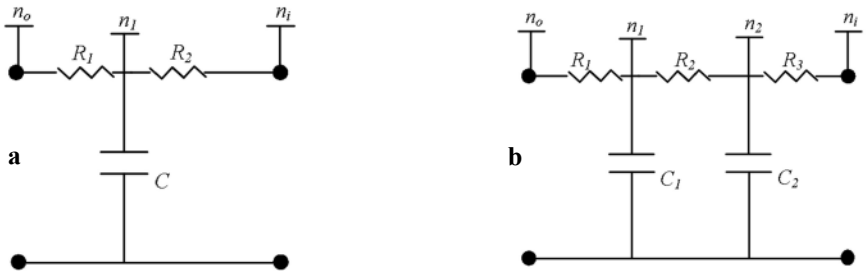

Figure 1 - a) Two resistors one capacitor LPM. When representing a single slab of material $R_1=R_2=0.5/(U\text{-}Value*Area)$. b) Three resistors two capacitors LPM.

Users of these models based in RC-networks, normally look to simplify the complete model to reduce the computation even if that implies losing some accuracy. Several works have looked into investigating ways of reducing complete large RC-networks into Lumped Parameter Models (LPM) (some examples are [12-16]).

Multi-layered constructions contribute largely to the overall size of RC-networks, so special interest has been seen in the literature in reducing constructions to low-order (few nodes) LPMs of multi-layered constructions ([15-17]).

Two approaches can be taken to find a LPM of a complete RC-network: a **numerical approach,** in which numerical methods are used to find the parameters that best approximate the complete RC-network [12, 15, 17], or, **analytical methods**, in which the equations of the RC-network are studied to obtain a set of algebraic equations that will provide the optimal LPM [13, 16]. Although the numerical approach normally finds the best LPM available for the given problem, it requires some previous information of the complete RC-network, such as its response in time or frequency. Also, the use of numerical methods to obtain the parameters implies a computational cost that might make the use of LPMs unattractive.

Only one method to find LPMs of multi-layered constructions using an analytical method has been found in the literature which reduces a multi-layered construction into a second order system consisting of three resistors and two capacitors (Fraisse et al.) [16]. However for some multi-layered constructions this methodology produces LPMs with low accuracy. In this paper we present a new analytic methodology to obtain LPMs of multi-layered constructions. Contrary to previous methods to obtain the reduced LPM, the method firstly is created without using transfer coefficients and secondly, it is built to be accurate in a range of frequencies that corresponds with the most significant frequencies of the inputs. The model presented is found to outperform the models created with the methodology of Fraisse et al for a wide range of constructions when they are used to simulate real constructions.

2 Method

2.1 Dynamic response of constructions: Range of relevant frequencies

The work presented in this paper focuses on finding a low-order model to represent multi-layered constructions. Multi-layered constructions are a superposition of layers of different materials. Each layer contributes to the dynamic response of the building and therefore, they have to be modelled as independent elements in the thermal model (addition of elements such as the one in Figure 1a forming an RC-network as the one in Figure 2). Modelling the layers independently makes the thermal model rather complex, hence the motivation to find a methodology that will reduce the number of elements in the thermal model that are needed to represent the thermal response of multi-layered constructions but keep the overall accuracy of the full model.

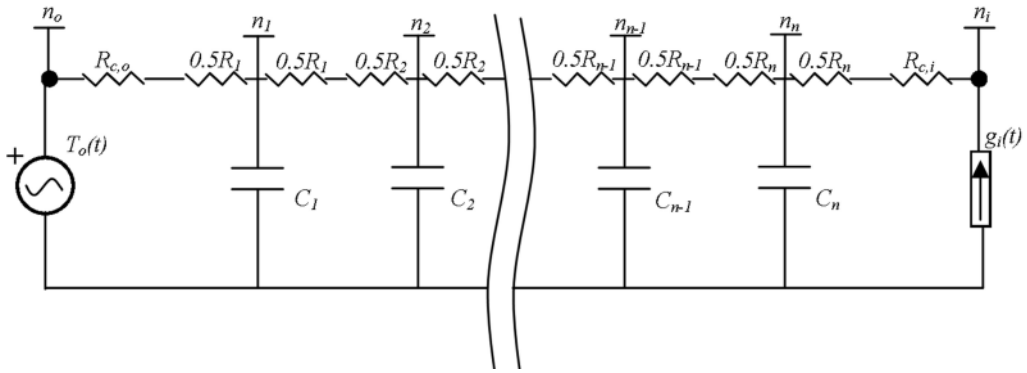

Figure 2 - RC network representing a construction with n layers subjected to a time-varying outside temperature, $T_o(t)$, and time-varying internal gains, $g_i(t)$. Note: the voltage source has been represented as sinusoidal, but it should be considered as a time series.

For the purpose of modelling buildings it is crucial that the reduced model is accurate under the normal operational conditions of a building. The main two boundary conditions of a construction used for the building envelope are: the outside ambient temperature which is applied to the most external layer of the construction (n_o in Figure 2), and the gains in the living space of the building (equivalent to n_i in Figure 2).

These two boundary conditions are time dependent, the outside temperature is read from a weather datafile, and the gains are generated *on-the-go* following occupant's patterns previously created by the user and heating requierements. The internal gains are therefore unknown before carrying out a dynamic simulation as the heating system is trigered by control mechanisms that read the internal temperature of the zone.

The first thing that was studied in our research was the range of frequencies of the inputs (outside temperature and internal gains). Every time series can be discompose into a set of harmonics with different frequencies (for example using the *Fast Fourier Transform*), if that is done with the inputs of the systems, one could obtain the frequencies of their main harmonics. A model of the construction that is accurate for those harmonics will be accurate in real-world simulations. Instead of considering individual harmonics, we have looked for a range of angular frequencies in which most of the harmonics of the inputs can be found. Creating a LPM that is accurate for that range was the aim of this research.

Firstly, the variables read from a weather data file were considered. Most dynamic simulators normally use data from weather files which contain a time-series of weather variables with one hour sampling period. Even though some simulators interpolate these time series, the Shannon-Nyquist theorem [18] established that a continuous function can be totally determined from a discrete time-series only if this original function has no harmonics higher than a frequency of half the sampling frequency (f_s) of the discrete series. This means that the continuous function from the discretized data can only be determined when it is assumed that the original function did not have harmonics with frequencies higher than half the sampling period. Harmonics higher than this value cannot be known from the interpretation of the sampled data as they are masked by the sampling. Under the assumption that these "fast" harmonics are not known. It has been assumed in this work that the accuracy of the model for those unknown higher frequencies is not relevant. As a result, it is possible to introduce an upper bound for the range of *relevant* frequencies given by:

$$f_{UB} = f_{SN} = 1/2T_s = 1/2\ h^{-1}\ ,\ and,\ \omega_{UB} = 2\pi f_{SN} = \pi\ rad\ h^{-1}\ , \quad (1)$$

where f_{UB} is the upper bound frequency, f_{SN} is the Shannon-Nyquist frequency, ω_{UB} is the upper bound angular frequency, and T_s is the sampling period.

This limit is justified for variables which are read from the weather data file which have a sampling period of one hour. However, the internal gains are generated on the go, and they can have other harmonics much higher than those equivalent to the ones with half an hour period. To verify that this upper bound of the range of angular frequencies is valid for the gains, a Fast Fourier Transform (FFT) has been applied to a time series of the internal gains obtained with EnergyPlus with a sampling period of one minute. The simulation performed included solar, electric and metabolic gains together with a heating system that is controlled by a thermostat. The results of this FFT can be seen in Figure 3.

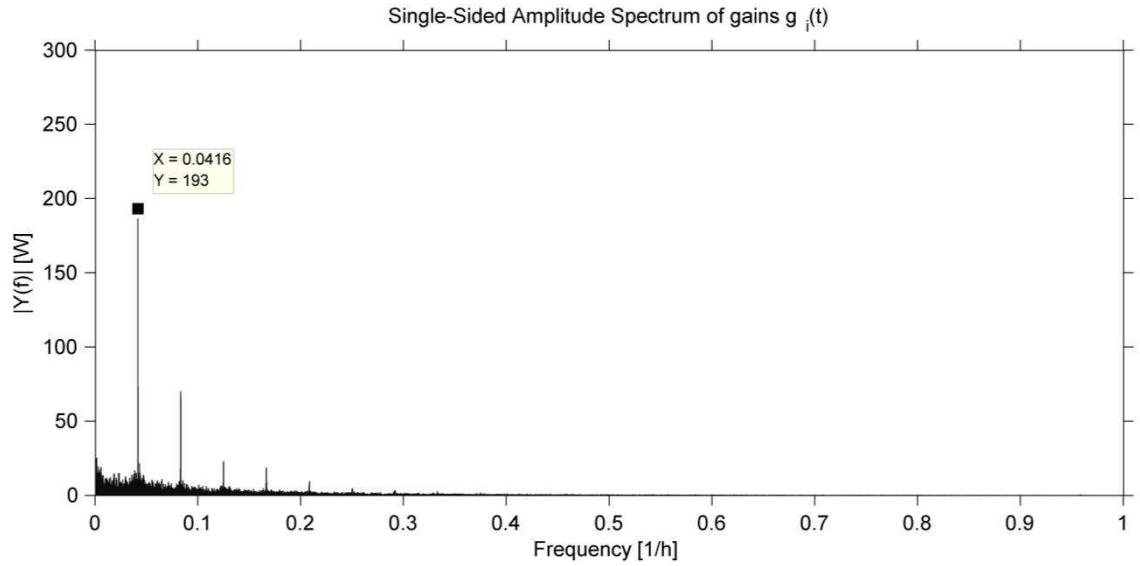

Figure 3 - Representation of the harmonics of a time series of internal gains in a building simulation (1 year) from data sampled at a resolution of 1 minute. Note: The peak representing the harmonic with the largest amplitude corresponds with the24 hour period.

The upper bound determined in the previous paragraph is conservative enough as there are no substantial harmonics for frequencies higher than 0.5 h^{-1} (equivalent to an angular frequency of: π rad/h) .

For the calculation of the lower bound, it is possible to use the physical properties of the construction. There are angular frequencies for which the construction will behave as in a steady state. The simplest method to obtain the order of magnitude of those frequencies is using the largest time constant of the system. The time constant is a measure of the time needed by the construction to react to a change in the input, and is calculated for each layer as the resistance multiplied by the capacitance ($\tau=RC$). Also, an angular frequency can be associated to this time constant, and that provides the angular frequency at which the system starts having dynamic effects (see [10]).

The equation that relates them is $\omega=1/\tau$ (with ω angular frequency and τ the time constant). If the largest time constant is considered, and the equivalent angular frequency obtained, then for any smaller angular frequency the system will have a steady state response. The lowest frequency, f_{LB}, considered is hence:

$$f_{LB}= 1/2\pi \ 1/(\sum_0^n R_k \ \sum_0^n C_k), \text{ and, } \omega_{LB}= 1/(\sum_0^n R_k \ \sum_0^n C_k), \quad (2)$$

where R_k is the resistance ($\propto$ 1/U-Value) of the k^{th} layer of the construction, n is the total number of layers, C_k is the thermal capacity of the k^{th} layer and ω_{LB} is the lower bound angular frequency.

With this, the range of relevant frequencies are determined by $[\omega_{UB}, \ \omega_{LB}]$, and the model will be constructed such that the maximun accuracy is achieved within this range.

2.2 Topology of the LPM

To obtain an LPM that represents the dynamic response of a construction, the topology of the model needs to be determined first. The first models that represented constructions dynamically were based on two resistors and one capacitor[19]. This topology of the LPM has been used by other authors and has shown to provide good results (e.g. [14]). However, more recent work has demonstrated the need for more complex models to represent constructions, especially those with larger thermal mass [17] [15]. The first order model assumes that the thermal capacity of the construction is contained in one single node; however, in most constructions, there is an intermediate layer with low thermal conductivity and low thermal capacity (insulation and/or air gap) which makes the dynamic response of the layers at either sides of this insulating layer rather independent. Gouda et al. proved the lack of accuracy of first order models of constructions [17], where the application of heat flow to the interior layer of the construction (the one in contact with the air of the zone, and therefore the one that receives the gains ultimatelly) highlights the deviation of the first order model from the complete model. The second order model (consisting of three resistors and two capacitors) has been found to provide a good compromise between accuracy of the response and complexity of the model [9,11].

2.3 The Dominant Layer Lumped Parameter Model

The linearity of the elements of the RC-network allows the application of superposition. We have considered the temperature of the internal surface of the construction, i.e. that which is in thermal contact with the internal air of the building (n_i in Figure 2) as the most interesting output of the dynamic system (the construction). When the dynamic model of the construction is considered, this internal temperature can be calculated as the sum of two responses from two models (or circuits): one with only outside air temperature as an input (T_o), and another with the only input being incidental/internal gains (g_i).

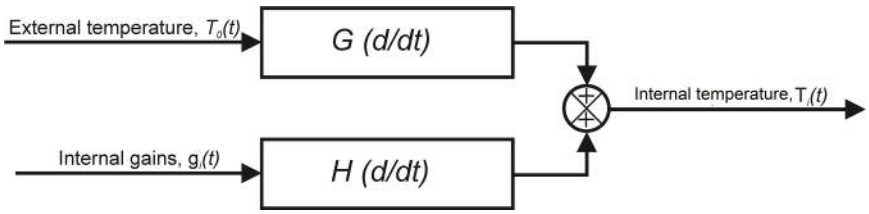

Figure 4. Internal temperature as the sum of the response of two linear systems.

Firstly, the model with incidental gains as the only input was considered (*H(d/dt)* in Figure 4). This model has a heat gain (or current source, see right side of Figure 2) applied to the node which represents the internal surface of the construction (n_i in Figure 2), and the node that represents the outer layer of the construction (n_o in Figure 2), is considered to be earthed, i.e. the outside temperature/voltage is set to zero.

The first equation of this system is obtained by considering steady-state conditions, for this, capacitors have infinite impedance and the circuit is reduced to a set of resistances in series. This produces the first requirement for the LPM:

$$\sum_{Construction} R_i = \sum_{LPM} R_j, \tag{3}$$

where R_i are the inverses of the conductivities of the different layers of the construction (i.e. $\propto$ 1/U-Value) and R_j the equivalent for the LPM.

The next equation to be derived will be obtained from studying the dynamic response of the system. To represent the dynamic behaviour of the construction the most significant dynamic characteristics of the complete network have to appear in the LPM. The cyclical nature of gains causes the heavy weight layers to have a much larger contribution to the dynamic response of the construction. If the construction is considered from the inside (from n_i to n_o), one is likely to find a layer of material that will store and release the majority of the heat during the repeated heating cycles. This *dominant layer* plays an important role in the dynamic response; the LPM presented in this paper is designed to represent this layer and therefore its effect on the dynamic response at the expense of other less important layers. The assumption will be that including this layer of material directly in the LPM will improve the accuracy.

The dominant layer is found from the consideration of the influence of each layer. The vertical branches of the circuit in Figure 2 represent the heat capacity of the layers within the construction. The impedance of each branch to the heat flow (i.e. the current) injected at the inner surface of the construction (the inside node n_i) could be considered as the impedance of the capacitor plus the sum of the resistances from the node of the branch to the inside node. This impedance varies with the frequency; however, we have created an *influence value* that is a measurement that averages the impedance for the range of angular frequencies previously defined (i.e. over the *relevant* range of angular frequencies, from ω_{LB} to ω_{UB}). The influence value (with units *h/(*Ω*rad)*) of each branch is defined as:

$$Inf_k = \left(\int_{\omega LB}^{\omega UB} \left(\left| 1/j\omega C_k + R_k/2 + \sum_{(j=k+1)}^{(n)} R_j \right|\right) d\omega\right)^{-1}, \tag{4}$$

where ω_{LB} and ω_{UB} are the lower and upper bound of the angular frequency, ω is the integration variable, j is the imaginary unit, R_k is the resistance of the k^{th} layer of the construction, n is the total number of layers, and C_k is the thermal capacity of the k^{th} layer.

The influence value of the branches is an indicator of the dominant layer; the higher its value, the larger the current that will pass through it, and thus, the impact of this branch on the dynamic response. The dominant layer is such that:

$$Inf_{dominant} = max_n \{Inf_k\}. \tag{5}$$

Identification of the dominant layer using Eq. (5) is the first step in the derivation of the LPM in our methodology as the contribution to the dynamic response from the layer is crucial. To include the dynamic effect of the dominant layer, the last capacitor and the last resistor (the ones in contact with the inside node) of the LPM are defined to represent the dominant layer. This is achieved by making the last capacitor of the LPM have the same value as the capacitance of the dominant layer and the last resistor of the LPM to have the same value as the sum of the resistances of the layers between the dominant layer and the inside node.

$$R_3 = 0.5*R_{dom} + \sum_{i=dom+1}^{n} R_i, \quad (7)$$

$$C_2 = C_{dom}, \quad (8)$$

with R_3 the third resistor of the DLM, C_2 the second capacitor of the DLM, *dom* the dominant layer, n the total number of layers, and R_i the resistance of layer i.

The explicit consideration of a dominant layer, as introduced in this paper, is the key element of the methodology; as such the LPMs obtained with this methodology have been called Dominant Layer Models (DLMs).

For the second model (or circuit, *G(d/dt)* in Figure 4), the time-varying outside temperature is incident on the node representing the external surface (n_o in Figure 2) of the construction and the internal gains are eliminated.

This RC-network is a set of T-networks (Figure 1a) in cascade, and each of those networks is a low pass filter as the input and output are respectively the voltage in the left and the right side of the T-network and each of the layers of material will stop high frequency changes of the outside temperature influencing the inside temperature.

It is therefore possible to calculate the *cut off* angular frequency for each layer which is given by $\omega_c = 1/RC$ or obtain the time constant $\tau=RC$ (where C is the capacitance of the layer of material and R is half of the resistance). However, the different layers are connected in cascade, and therefore, each of the layers will have a resistance from the other layers on both sides (except for the external layers). According with the methodology of Matthews et al. [13], one can calculate two time constants for each of the layers that will relate with the cut off angular frequencies from the inside and from the outside (n_i and n_o respectively in Figure 2). The time constant of each layer for the outside (τ_{os}) is therefore calculated by summing all the resistors previous to the layer (from the outside in) and multiplying them by the capacitor of the layer, and the time constant for the inside (τ_{is}) is calculated by summing all the resistors after the layer (from the outside in) and multiplying them by the capacitor of the layer.

However, the dominant layer has already been included in the LPM, so the relevant first-order model (Figure 1a) ignores the layers which have taken into account by the dominant layer, being this the ones between the dominant layer and the last layer adjacent to the zone. We have assumed that due to the nature of the RC-network resultant when using outside temperature as single output, the first order model will be able to produce accurate responses in conjunction to the resistors and capacitor defined to represent the dominant layer, the result is a LPM with the topology shown in Figure 1b.

Matthews et al. showed that the most accurate first order model for the outside temperature can be obtained calculating the summation of the time constants from the inside and outside of each layer. As the dominant layer

and the layers after this (from the outside in) are already in the LPM, the equation to calculate the summation of the time constants will be:

$$\tau_{is}=\sum_{(j=1)}^{(dom-1)} C_j \left(R_j/2+R_{dom}/2 \sum_{(k=j+1)}^{(dom-1)} R_k \right) \text{ and} \quad (9)$$

$$\tau_{os}=\sum_{(j=1)}^{(dom-1)} C_j \left(R_j/2+\sum_{(k=1)}^{(j-1)} R_k\right), \quad (10)$$

where τ_{is} and τ_{os} are the time constants relative to the two sides of the circuit (inside and outside respectively) and C_j and R_k are the capacity and the resistance of the j^{th} and k^{th} layer respectively and *dom* represents the position of the dominant layer starting from the outside. The summation of the time constants has to be equal to the time constants of the first order model. Therefore the following equations can be written:

$$R_1 = (R_t' * \tau_{os})/(\tau_{is} + \tau_{os}), \quad (11)$$

$$R_2 = (R_t' * \tau_{is})/(\tau_{is} + \tau_{os}), \quad (12)$$

$$C_1 = \tau_{os}/R_1 = \tau_{is}/R_2, \quad (13)$$

There are now two equations that together with the steady state conditions and the dominant layer will determine completely the LPM. Although the topology of the DLM is the same as that developed by the work of Gouda and Xu among others ([15-17, 20]); in opposition to those, the methodology presented in this paper does not explicitly include a requirement that forces the total capacitance of the LPM to be equal to the total capacitance of the model of the whole construction.

2.4 Summary of the DLM

Given the topology of the simple model defined by Figure 1(b), it is straightforward to obtain the parameters of the simplified model for a given construction:

1. Find the dominant layer using Eq. (5) and (6).
2. Assign the capacitance of the dominant layer to C_2.
3. Obtain R_3 with Eq. (7).
4. Obtain R_1 with Eq (11).
5. Obtain R_2 with Eq (12).
6. Calculate C_2 with Eq. (13).

3 Validation

For numeric modelling, a simplified model has the aim of representing real constructions while reducing the computational time. To demonstrate the accuracy of the DLM, six constructions have been modelled creating the RC-networks that represent each multi-layered construction.

The layers of material used in the test constructions were transformed to T-networks as seen in Table 1. The constructions are defined in Table 2. This table shows that the constructions used to validate the method have similar materials and topologies to those in real buildings, except for the last two (*proof* and *all heavy*).These were included to check the method accuracy in extreme cases.

Fraisse presented a way of obtaining the parameters of a LPM with the same topology as the DLM, also in an analytical way, but using a different method [16]. As the DLM is an alternative to Fraisse's approach, the two are compared in the following. Although Fraisse's methodology uses an analytical approach, it must be noted that the computational time to obtain the DLM is shorter and the method more intuitive.

Table 1 - Resistance and heat capacitance values for a $1m^2$ layer of the materials used.

Material	Thickness (mm)	Resistance (K/W)	Capacitance (Wh/K)
Air gap	n/a	0.1500	n/a
Brick	101.6	0.1142	42.80
Concrete	300	0.1538	168.0
Gypsum	19	0.1187	4.602
Insulation	125	4.1667	1.806

Table 2- Constructions.

Light	Outside – gypsum – insulation – gypsum – Inside
Heavy	O. – brick – ins. – concrete – gypsum – I.
Sandwich1	O. – brick – air – brick – I.
Sandwich2	O. – brick – air – brick – insulation – I.
Proof	O. – gypsum – ins. – gypsum – conc. – gypsum – brick – air – brick – gypsum – I.
All heavy	O. – gypsum – conc. – gypsum – brick – conc. – brick – gypsum – I.

To evaluate the accuracy of the DLM, Bode diagrams and time-domain responses were generated. Bode diagrams represent the relationship between the outputs and the inputs in different frequencies in magnitude and phase. The Bode diagram of magnitude shows how much the input will be amplified or reduced at the output location depending on the frequency of the input. The Bode diagram of phase shows the lag between an oscillation at the input and the corresponding response at the output depending on the frequency of the input, (for more information about Bode diagrams and frequency response of dynamic systems see [10]).

It was described before that the response of the construction can be studied independently affected only by outside temperature of only by internal gains. The accuracy of the reduction method presented in this paper has been tested for both inputs separately. The response (internal temperature) was analysed under outside temperature (T_o), and internal gains (g_i). The results are two separate sets of Bode diagrams like the ones in Figure 5. After that, the accuracy of the models under both inputs was tested in the time domain.

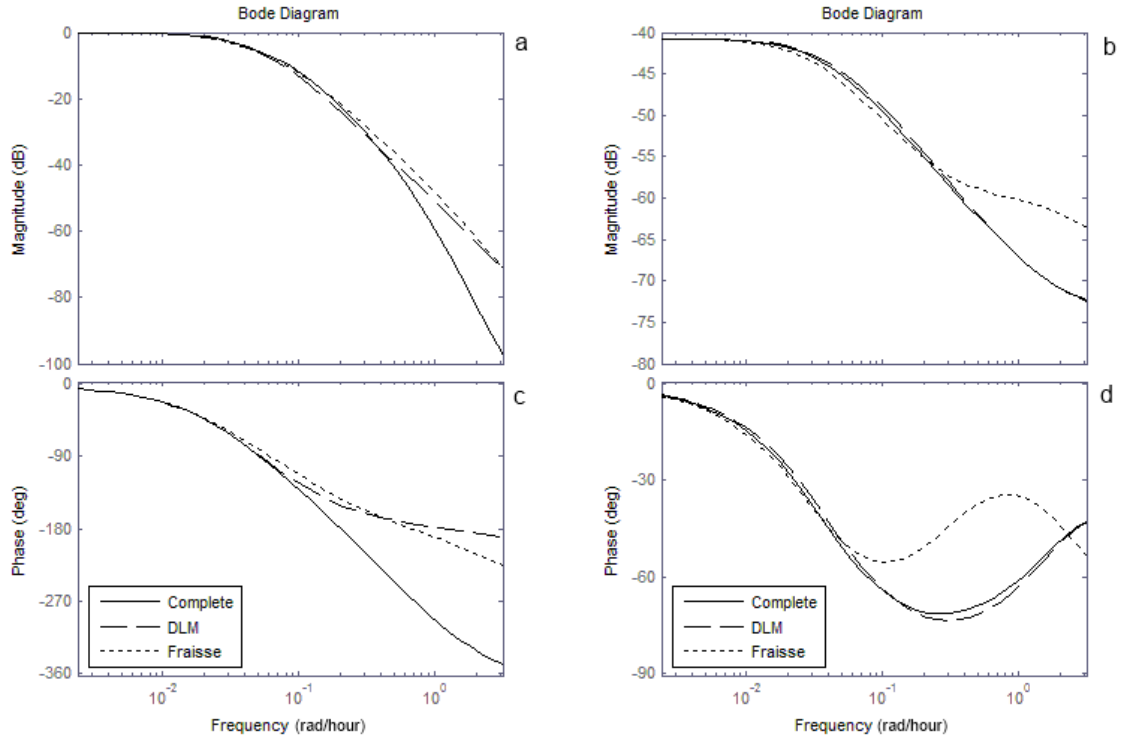

Figure 5 - Example Bode diagram for the construction named *sandwich 2*. Input: external temperature (T_o) (left pair); internal gains (g_i) (right pair). Solid line: complete model; dashed: DLM; points: LPM obtained with Fraisse's method.

4 Results and discussion

Figure 5 shows example Bode diagrams comparing the complete model with the DLM and the LPM with parameters obtained by Fraisse's methodology. In plots *a* and *c* of Figure 5 the system is driven by a sinusoidal varying outside temperature; in plots *b* and *d* by sinusoidal varying internal gain. These bode diagrams were obtained for every construction. However, for simplicity, the discrepancy in these diagrams has been shown by the values of the curves at the angular frequency at which the differences between models are largest. For example Figure 5 shows that Bode diagrams present the maximal differences at 3.14 rad/h for diagram *a*; two pair of bars will be shown with values: -97.4 (complete) with -71.3 (DLM) and -97.4 (complete) with -71.3 (Fraisse). That shows that both models are similar for this construction. When representing the plot *d*, the values will be shown as two pairs of bars with values: -68.8 (complete) with -71.4 (DLM) at frequency 0.52 rad/hour and -68.8(complete) with -36.8 at the same frequency. For this case the DLM clearly outperforms Fraisse's model and so is shown in the bar diagrams (Figures 6 and 7 construction *sandwich 2*).

The first response studied in the frequency domain was under outside temperature.

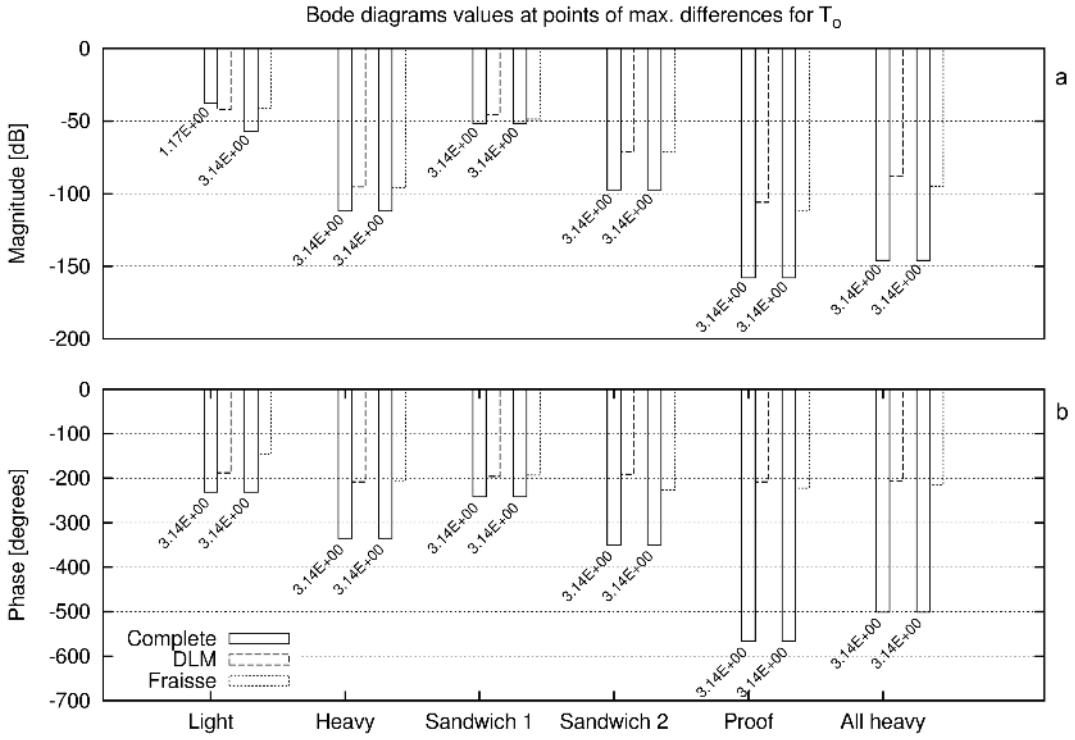

Figure 6 - Values of magnitude and phase for the three models when using T_o as input. The pairs of bars show the value of the Bode diagram for the complete and the reduce model (DLM or Fraisse's) and the angular frequency at which the maximum difference is found (the angular frequency is in rad/hour).

Figure 6 shows pairs of bars representing the values of the curves in the Bode diagrams at which the differences between the complete model and the DLM and the Fraisse model were the largest. The plot has been generated for the six constructions and for magnitude and phase, considering T_o as the input. The number under the bars represents the angular frequency at which the maximum difference is found.

The first conclusion from Figure 6 is the fact that, in the magnitude plot, the values are large. A magnitude value of 100dB in the Bode diagram represents a reduction by a factor of 10^5. As an example: if the construction *sandwich 2* is considered, it is seen that the value of magnitude at which the maximum difference is found is around 100 dB. A change of outside temperature of 1 degree, will contribute to a change in internal temperature in: 10^{-5} degrees, what can be considered negligible for a building simulation. Performing the comparison between the two models (completed and any of the LPM) for the same example (*sandwich 2*), a change of temperature in the outside temperature of one degree is translated in a change in inside temperature of $10^{-4.87}$ degrees for the complete model and $10^{-3.56}$ degrees for the DLM or Fraisse's model, this implies an absolute difference of: 0.000262 degrees for the worst case scenario.

If one considers the construction *light*, as it has the smallest attenuation of the input; 1 degree oscillation at the angular frequency of Figure 6a will lead to: $10^{-2.85}$ degrees for the complete model and $10^{-2.06}$ degrees for Fraisse's model in internal temperature, this results in an absolute difference of 0.00730 degrees. Therefore, the differences seen in these Bode diagrams are substantial, but they occur at frequencies where the response have been reduced enough to be considered negligible.

The graph in Figure 6a also shows that the models generated with the DLM have in general the same differences with the complete model as the ones generated with Fraisse's methodology, only in constructions *sandwich 1, proof* and *all heavy* the model created with Fraisse's methodology have smaller error than the DLM (with a difference between the two of: 6.07%, 3.68% and 4.72% respectively). The DLM outperforms the model created with Fraisse's method for construction *light*, with the difference between complete and reduced model of 27.65% for this method and 10.91% for the DLM.

Figure 6b shows the values of the bode plot of phase at which the differences were the largest. As in Figure 6a, the deviations for both Fraisse's and the DLM with respect to the complete model are similar. The only construction that produces a significant difference is *light*. For this construction the DLM shows a smallest maximum difference with the complete model than the model created with Fraisse's methodology. However, it can be seen that for constructions *Sandwich 2*, *proof* and *all heavy*, Fraisse's model is slightly better than the DLM, with relative improvement over the DLM of 9.75%, 2.57% and 1.28% respectively over the complete model. The difference between the two in *heavy* and *sandwich 1* are negligible and for *light*, the DLM is an 18%closer to the complete model than Fraisse's model. The impact of these discrepancies in real simulation (time-domain) will be studied further in this section.

Figure 6 shows that the differences in the Bode diagrams of the complete and the reduced models can be large. However, the maximum differences are found at points where the input has been reduced largely. It will be shown that because of this differences happening when the inputs are negligible, the reduced models perform well despite their limitations.

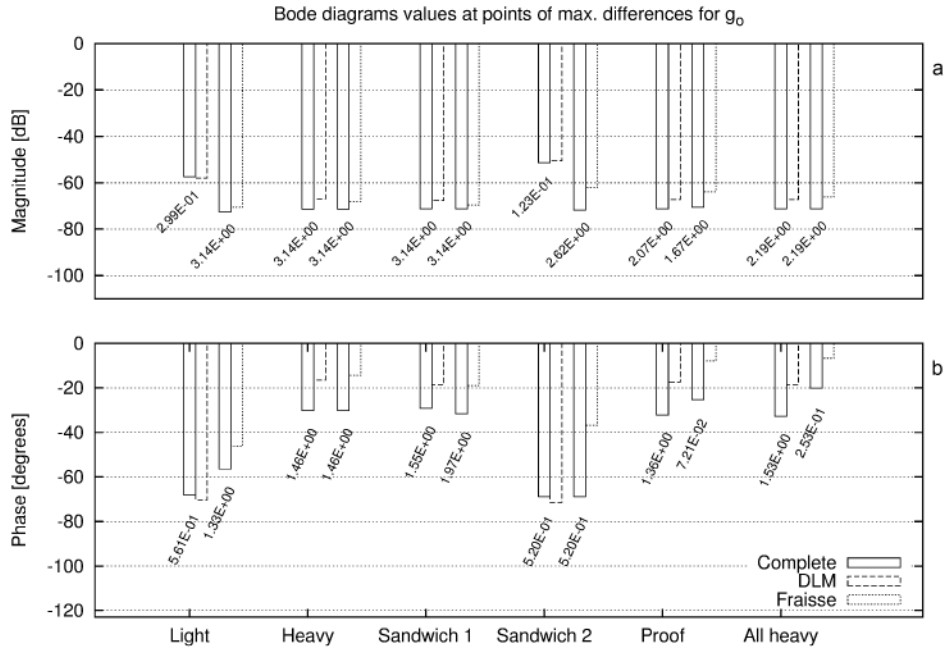

Figure 7 - Values of magnitude and phase for the three models when using g_i as input. The pairs of bars show the value of the Bode diagram for the complete and the reduce model (DLM or Fraisse's) and the angular frequency at which the maximum difference is found (the angular frequency is in rad/hour).

The graph in Figure 7 shows the values of the curves of the Bode diagrams at which the differences between the three models were largest. The DLM equals or outperforms Fraisse's model in almost all constructions. Although the order of the magnitude plot (Figure 7b) implies a reduction of the input as high as the one shown by Figure 6a, one should consider that the input for this graphs (internal gains) has variations that are normally between one to two orders of magnitude larger than variations in outside temperature (see the profile of realistic gains and outside temperature in Figure 8).

Under gains, the magnitude bode diagrams of the DLM are similar to those of the complete model. The reduced model generated with Fraisse's method outperform the DLM in constructions *heavy* and *sandwich 1* by a small amount (1.53% and 2.62% respectively). The Fraisse method works well for most constructions in magnitude. However, the error for construction *Sandwich 2* is larger than in any other with a 13.5% deviation.

Figure 7b shows the value of the Bode diagrams where the largest differences are found between models. Constructions *light* and *sandwich 2* show a substantial difference between the complete model and Fraisse's model, the difference is smaller than the difference between the complete model and the DLM. For constructions *heavy, sandwich1, proof* and *all heavy,* the reduced models are not able to follow accurately the complete model and that is shown in substantial differences in the Bode diagrams of the reduced and the complete models. Although both models show substantial differences the DLM outperform the Fraisse's model in constructions *proof* and *all heavy*.

After comparing the discrepancies in the frequency domain, three periods of 48 hours have been simulated in the time domain, to show the implication of the disparities in the bode diagrams are in the time-domain response. The three periods are from 100 to 148 hours, from 2000 to 2048 hours and from 4000 to 4048 hours with this we aim to visualise the response in winter, spring and summer to show the accuracy of the models for three different periods of weather. This is relevant because the resistances taken in the models based in RC-networks to represent convection and radiation were fixed, and we know that those will take different values depending on the weather conditions. The constructions were used to create a simplistic building model consisting on a box of 10x10x5m that was simulated with the outside temperature given by a weather file of London [21] and a modulating realistic gain (see Figure 8). With this, it is possible to visualise the effect of the discrepancies in the Bode diagrams (previously shown) in the simulations carried out in the time domain.

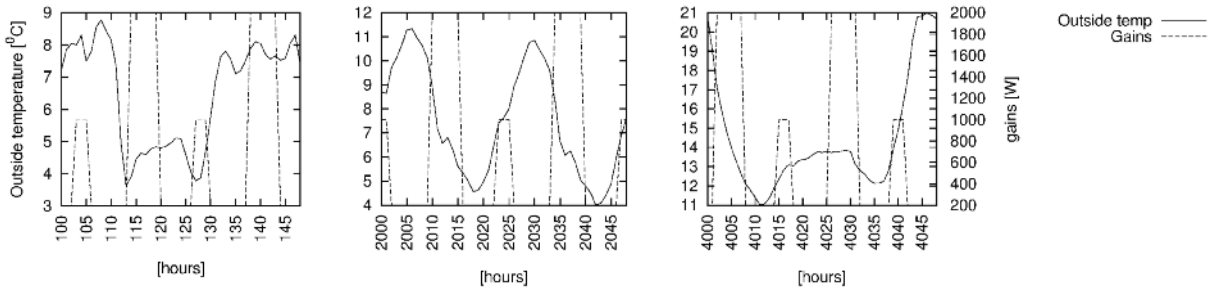

Figure 8 - Inputs of the dynamic models. Outside temperature and heat flow for three 48 hours periods in winter, spring and summer.

A series of figures have been generated with the temporal responses from the simulations described in the previous paragraph. However, to reduce the number of figures, only the most significant have been included in

the paper. In these simulations, the response using EnergyPlus was included as a reference. The starting temperature for the dynamic simulation has been adjusted to be the same as the one in the EnergyPlus simulation. Three periods of 48 hours in winter spring and summer has been selected to show the accuracy of the different models.

The bar diagrams in Figure 6 and 7 show little difference in the frequency domain between the models (complete, DLM, Fraisse's) for the construction *light*. Figure 9 illustrates the similarity of the responses of the different models in the time domain.

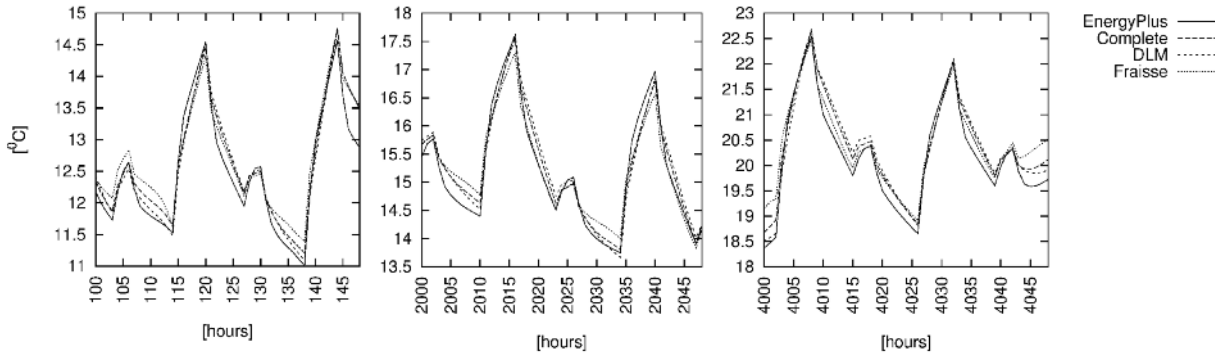

Figure 9 - Temporal response for the model when using that use the construction "Light".

The internal temperature of the construction *light* under the input in Figure 8 is shown in Figure 9. The responses of the three models and EnergyPlus are in general similar. It should be noted that Fraisse's model seems to over predict the response slightly. This difference is particularly noticeable around the periods 2025-2035 hours and 4045-4048 hours. These differences could be related to the significant difference found in Figure 7 in phase for this construction, but in general the differences are small.

Similar to Figure 9 were the plots of the responses of the three models representing constructions *heavy* and *sandwich 1*. In the three plots, there is a clear difference between the output of EnergyPlus and the outputs of any of the models based in RC-networks. This shows that the biggest lack of accuracy in these cases is introduced by phenomena that are not taken into account in the models based in RC-networks (non-linear phenomena such as radiation and convection). However, the response of the models based in RC-networks is similar despite the fact that there are small differences in the Bode diagrams of these construction. For the first three constructions, the internal gains seem to have the same effect in the three models as there are no clear differences with respect to the heating cycles. Although some differences were observed in the frequency domain of the three models representing these constructions, the discrepancies seem not to influence in the temporal response of the models greatly.

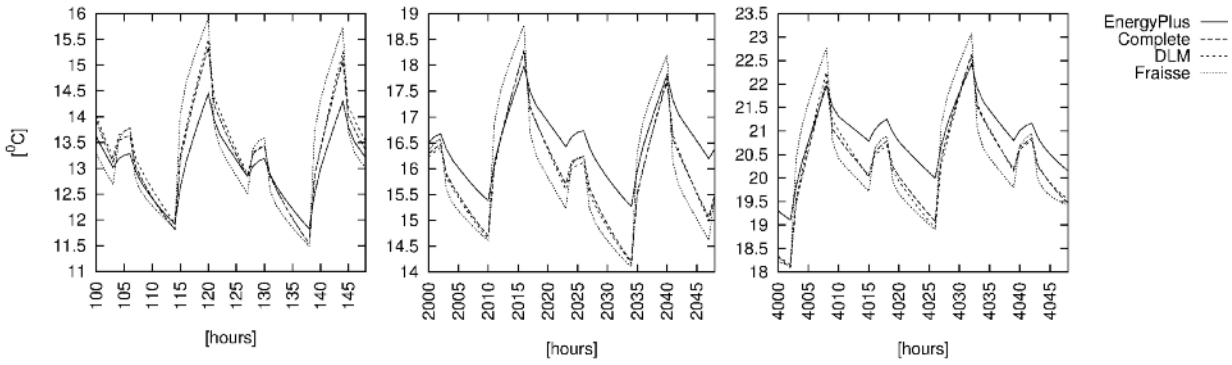

Figure 10 - Temporal response for the model when using construction "Sandwich 2".

The temporal response of *sandwich 2* has been shown in Figure 10. The response of the models in this case highlights a higher accuracy of the DLM compared with Fraisse's model. This lack of accuracy seems to be particularly visible in the heating cycles. This is because of the lack of accuracy of the construction under gains using the Fraisse methodology. As shown by Figure 7, this construction shows the highest difference between complete and Fraisse's model for phase under g_i. The angular frequency at which the highest difference is found is one of the lowest at 0.52 rad/hour (close to the angular frequency for the daily cycle: 0.26 rad/hour), making this difference in the Bode diagram more influential in the time domain under realistic inputs.

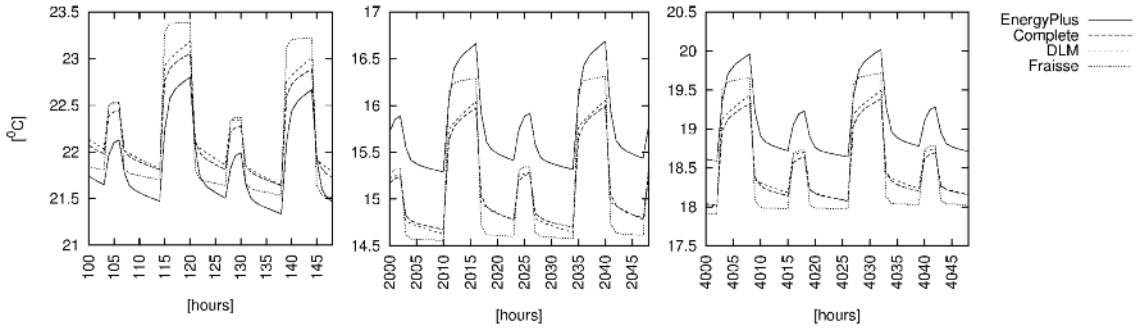

Figure 11 - Temporal response for the model when using construction "Proof".

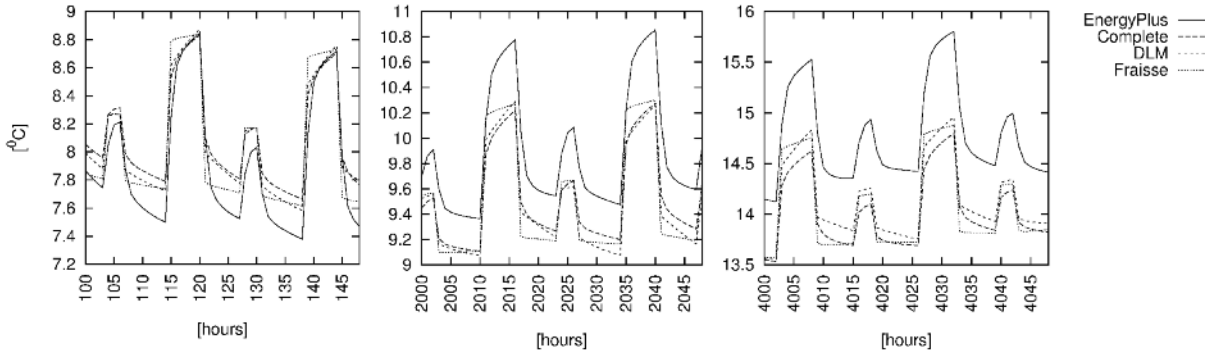

Figure 12 - Temporal response for the model when using construction "All heavy".

Figure 11 and Figure 12 show the temporal response to the constructions *proof* and *all heavy*. The differences from the Bode diagrams predict an overestimation of the effect of the heating cycles in the internal temperature for construction *proof*, and *all heavy* using the model obtained with Fraisse's method. The differences between the Bode diagrams are found at low angular frequencies in the case of the model generated with Fraisse's methodology (0.072 rad/ hour and 0.25 rad/hour for *proof* and *all heavy* respectively), this implies a lack of accuracy in the representation of the internal temperature under the heating cycles, the shape of the curve that represents the internal temperature in these two cases is inaccurate using Fraisse's model. The DLMs for these two constructions are accurate when compared with the complete model; this improvement in accuracy under internal gains is much larger than the reduction of accuracy of the models under outside temperature (see Figure 6). The response of the DLM is very accurate in the construction *proof*. However, the DLM for the construction *all heavy* seems to lose accuracy in the third period (summer) and the outputs becomes as inaccurate as the output from Fraisse's model, although the DLM outperforms Fraisse's model for winter and spring. This lack of accuracy in this specific period shows a lack of consistency in the accuracy of the DLM, although it is not seen that the DLM produce a response in the time domain that is worse than a response from Fraisse's model.

5 Conclusions

This work shows the possibility of reducing complex thermal networks representing multi-layered constructions to a second order dynamic model by the application of a very simple set of rules. The method has been conceived to generate models that have the highest accuracy under the normal operation of buildings i.e. generating an accurate response under outside temperature and internal gains.

The models obtained with this methodology have been studied, in the frequency domain, and in the time domain. All models have been compared with the alternative found in the literature [22] to verify the advantages of the proposed methodology. To check the accuracy of the models four constructions have been defined similar to those used in real buildings; also, two complex constructions have been generated to check how scalable the methodologies are.

The reduced models (the one presented in this paper and the alternative found in the literature) are able to represent the complete models (truly representing all the layers of the construction) well in most cases. However, the methodology found in the literature [16] can generate outputs that are not accurate enough when used to model some of the example constructions.

The DLM, generates outputs in the time domain that equals or outperform in accuracy the models created with Fraisse's methodology. This is particularly the case when the constructions have a large number of layers or substantial levels of intermediate insulation. This shows that the scalability of Fraisse's method is poor, and that walls with intermediate insulation (that might become more common due to energy efficiency measures) should not be represented with these models.

The studies in the frequency response of the models of the partitions are useful to understand the accuracy of the models, especially considering the accuracy of the models at frequencies close to the frequency equivalent to the daily cycle. The cyclical nature of the conditions in a building (such as outside temperature and gains) makes it very important to generate models which are accurate for these specific frequencies (as was done by [22]).The method presented shows that giving importance to the accuracy of the models at those frequencies is more

relevant than calculating transfer coefficients that are “blind” to the importance of each frequency in a building simulation.

The methodology presented here fixed the model to be accurate for the internal gains first, and this estimates the value of the rest of the components to make it accurate for outside temperature. This has been seen to be favourable, and produce good results, especially when constructions are more complex or have more insulation. Due to the general trend of building more efficient houses, the methodology presented in this paper should be adopted for obtaining reduced models of multi-layered constructions to secure more accurate results.

The need to accurately model the dynamic behaviour of the constructions makes up a significant proportion of the computational time in a whole-building simulation; being able to reduce this computational time will allow models that run multiple representations of a design, or of driving forces, to be completed more rapidly; for example in automatic optimisation algorithms [23].

Summarising, the methodology presented in this paper:

- Proofs that second order linear LPMs can represent complex multi-layered constructions (tested with up to nine layers in this paper).
- Shows that a range of frequencies can be found that will delimit most of the harmonics obtained after applying an FFT to the outside temperature and the internal gains of buildings.
- Shows that a method that takes into account the operational conditions of buildings is more accurate than using transfer coefficients to reduce the model.
- Shows that a simple set of analytic rules is enough to define a LPM of a construction.
- Shows that producing a LPM that is accurate in representing the effect of internal gains in the internal temperature is important for the overall accuracy of the model.

6 Acknowledgement

Alfonso P. Ramallo González would like to thank the Wates Family Enterprise Trust and Matthew E. Eames would like to thank the EPSRC (grant ref EP/J002380/1) for their support.

7 References

1. DECC, *Digest of United Kingdom Energy Statistics*, 2011, Department of Energy and Climate Change: London.
2. Boardman, B., *Home truths: A low-carbon strategy to reduce UK housing emissions by 80% by 2050*, U.o. Oxford, Editor 2007, University of Oxford's Environmental Change Institute: Oxford.
3. Crawley, D.B., et al., *Contrasting the capabilities of building energy performance simulation programs.* Building and Environment, 2008. **43**(4): p. 661-673.
4. Magnier, L. and F. Haghighat, *Multiobjective optimization of building design using TRNSYS simulations, genetic algorithm, and Artificial Neural Network.* Building and Environment, 2010. **45**(3): p. 739-746.
5. Coley, D.A. and S. Schukat, *Low-energy design: combining computer-based optimisation and human judgement.* Building and Environment, 2002. **37**(12): p. 1241-1247.
6. Kämpf, J.H. and D. Robinson, *A hybrid CMA-ES and HDE optimisation algorithm with application to solar energy potential.* Applied Soft Computing, 2009. **9**(2): p. 738-745.
7. Kershaw, T., M. Eames, and D. Coley, *Assessing the risk of climate change for buildings: A comparison between multi-year and probabilistic reference year simulations.* Building and Environment, 2011. **46**(6): p. 1303-1308.
8. Clarke, J., *Energy Simulation in Building Design*2001: Taylor & Francis.
9. Balcomb, J.D., J.C. Hedstrom, and R.D. Mcfarland, *Simulation Analysis of Passive Solar Heated Buildings - Preliminary-Results.* Solar Energy, 1977. **19**(3): p. 277-282.
10. Ogata, K., *Modern Control Engineering*2002: Prentice Hall.
11. Barbaro, S., C. Giaconia, and A. Orioli, *Analysis of the accuracy in modelling of transient heat conduction in plane slabs.* Building and Environment, 1986. **21**(2): p. 81-87.
12. Coley, D.A. and J.M. Penman, *2nd-Order System-Identification in the Thermal Response of Real Buildings .2. Recursive Formulation for Online Building Energy Management and Control.* Building and Environment, 1992. **27**(3): p. 269-277.
13. Mathews, E.H., P.G. Richards, and C. Lombard, *A First-Order Thermal-Model for Building Design.* Energy and Buildings, 1994. **21**(2): p. 133-145.
14. Gouda, M.M., S. Danaher, and C.P. Underwood, *Low-order model for the simulation of a building and its heating system.* Building Services Engineering Research and Technology, 2000. **21**(3): p. 199-208.
15. Xu, X.H. and S.W. Wang, *Optimal simplified thermal models of building envelope based on frequency domain regression using genetic algorithm.* Energy and Buildings, 2007. **39**(5): p. 525-536.
16. Fraisse, G., et al., *Development of a simplified and accurate building model based on electrical analogy.* Energy and Buildings, 2002. **34**(10): p. 1017-1031.
17. Gouda, M.M., S. Danaher, and C.P. Underwood, *Building thermal model reduction using nonlinear constrained optimization.* Building and Environment, 2002. **37**(12): p. 1255-1265.
18. Shannon, C.E., *Communication in the presence of noise (Reprinted from the Proceedings of the IRE, vol 37, pg 10-21, 1949).* Proceedings of the Ieee, 1998. **86**(2): p. 447-457.
19. Lorenz, F. and G. Masy, *Methode d'evaluation de l'economie d'energie apportee par l'intermittence de chauffage dans les batiments. Traitment par differences finies d'un model a deux constantes de temps.*, 1982 (in French), Faculte des Sciences Appliquees, University of Liege.
20. Goyal, S. and P. Barooah. *A Method for model-reduction of nonlinear building thermal dynamics*. in *American Control Conference (ACC), 2011*. 2011.

21. DoE, *London-Gatwick, weather datafile*, U.S.D.o. Energy, Editor 2011, http://apps1.eere.energy.gov/buildings/energyplus/cfm/weather_data3.cfm/region=6_europe_wmo_region_6/country=GBR/cname=United%20Kingdom.
22. Tindale, A., *Third-order lumped-parameter simulation method.* Building Services Engineering Research and Technology, 1993. **14**(3): p. 87-97.
23. Peippo, K., P.D. Lund, and E. Vartiainen, *Multivariate optimization of design trade-offs for solar low energy buildings.* Energy and Buildings, 1999. **29**(2): p. 189-205.